RECENT PHOTOPRODUCTION RESULTS FROM THE FERMILAB BROAD BAND BEAM

Michael F. Gormley
Fermi National Accelerator Laboratory
Batavia, Illinois 60510 USA

Summary

As the title indicates, this talk will concentrate primarily on a review of new results on photoproduction reactions obtained with the Fermilab broad band beam since the Hamburg conference of two years ago. Some related low energy results from Cornell and Daresbury are also summarized. The photoproduced mass spectra of $\pi^+\pi^-$ and $\bar{p}p$ final states is presented and examined for possible evidence of resonant structure and new results on the two body decays of the $\rho'(1600)$ are described. An analysis of the photoproduced 4π and $KK\pi\pi$ final states is described and the evidence for excited recurrences of the ρ and ϕ is summarized. The four body final states containing two kaons are also examined for evidence of new massive mesonic states and their relationship to the quark-line (Okubo-Zweig-Iizuka) rule is summarized. The results of a search for charmed meson production is described and the cross section for photoproduction of $D^0(\bar{D}^0)$ mesons is reported.

Beam and Detector Layout

The broad band neutral beam at Fermilab has been described in several proceedings [1,2]. The single, most distinguishing feature of this beam is the photon energy spectrum which is displayed in Figure 1.

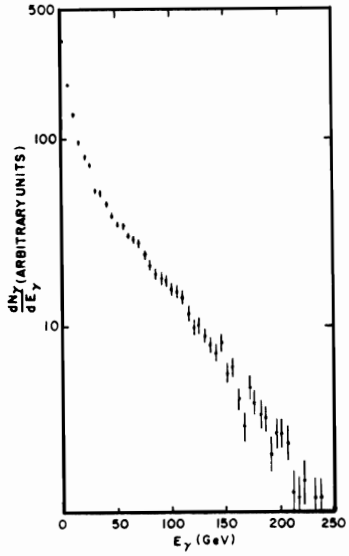

Fig. 1. Energy spectrum of photons in the broad band beam.

The detector layout used with the broad band beam has experienced a thorough upgrading over the last two years. A brief description of the experimental layout, shown in Figure 2, will emphasize those improvements which are especially important for the physics results presented here.

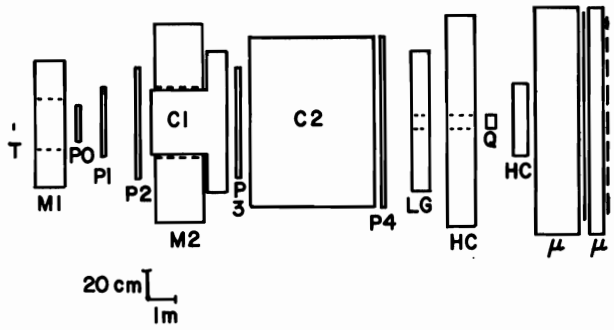

Fig. 2. Experimental layout for Fermilab photoproduction experiment.

The detector consists of a magnetic spectrometer, which makes use of two magnets (M1, M2), and five proportional wire chambers (PO-P4), supplemented by two Cerenkov counters (C1, C2), a lead glass array (LG), a muon identifier (μH, μV), and a hadron calorimeter (HC) to provide relatively complete particle identification. The first three proportional chambers have active areas much larger than the aperture of either magnet so that low-momentum, large-angle tracks which traverse only the first three chambers are reconstructed just as successfully as tracks which traverse the entire spectrometer. In each proportional wire plane, bands of either eight or sixteen wires are ganged together and connected to drift time digitizers. The measured drift times result in improving the position resolution by a factor of between two and three - a significant enchancement in searching for narrow resonances.

The primary particle identification system makes use of two, multi-cell, threshold Cerenkov counters filled with gas at atmospheric pressure. The active volume of the first Cerenkov counter, C1, is filled with nitrogen and completely occupies the aperture of magnet M2. This counter possesses twelve individual cells, each with its own phototube, and has a pion threshold of 6 GeV/c. The second Cerenkov counter, C2, is situated between the last two proportional chambers and contains a 4.7 meter long gas radiator which is a 20% nitrogen, 80% helium mixture. C2 has sixteen individual cells and possesses a pion threshold of 11 GeV/c. The large number of cells in these two counters is pivotal in separating kaons and protons from pions in high-multiplicity final states.

Two-Body Final States

Two-Pion State

The results of a recent measurement on the energy dependence of the rho photoproduction cross section have been summarized by the previous speaker.[3] Typical momentum transfer distributions and a typical two pion mass spectrum for this process are shown in Figure 3.

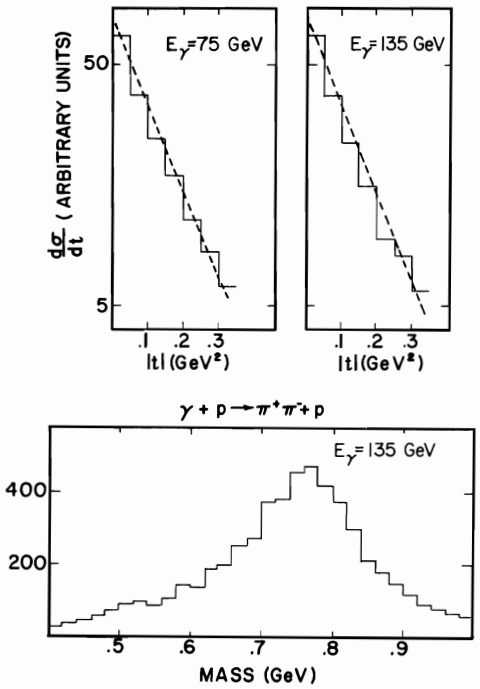

Fig. 3. Typical dipion mass spectrum and momentum transfer distributions for high energy rho photoproduction.

The $\pi^+\pi^-$ mass spectrum produced by 135 GeV photons possesses all the properties that have become familiar from the low energy data, e.g. the ρ^0 shape is clearly skewed toward lower masses compared to a p-wave Briet-Wigner resonance shape. The slope of the momentum transfer distribution appears to be independent of energy over the range from 50-150 GeV. This result confirms the assumption made by Eisner in unfolding the data from the tagged photon experiment.[3] The dashed curves in Figure 3 are a linear average of the slope parameters obtained from $\pi^+ p$ and $\pi^- p$ elastic scattering at the appropriate energy. The agreement between the photoproduction results and the prediction of the additive quark model is excellent for momentum transfers less than 0.4 GeV^2.

The photoproduced $\pi^+\pi^-$ mass spectrum above 1.0 GeV has always been an interesting region to examine for the existence of higher mass isovector states. This high mass region has been analyzed recently using data taken in the broad band beam with a nuclear target (Carbon). The distribution of events as a function of p_T^2 (p_T=transverse momentum) is shown in Figure 4 for all dipion events with masses greater than 1.0 GeV.

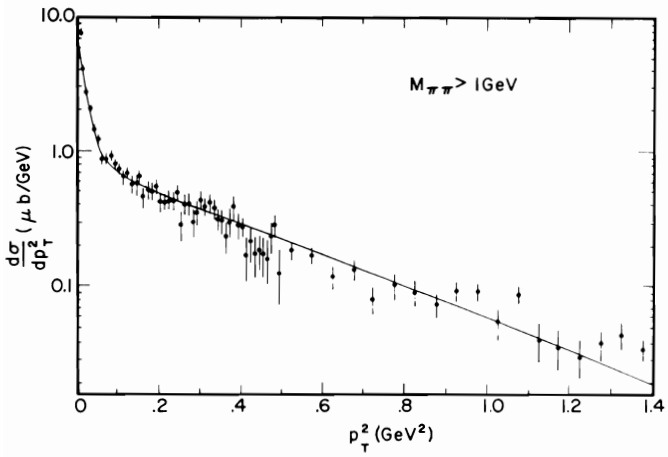

Fig. 4. The p_T^2 distribution for exclusively produced two pion final states with masses > 1.0 GeV.

The distribution shows the very strong forward peaking characteristic of diffractive photoproduction from a nuclear target. The solid curve represents the result of fitting the distribution to the sum of two exponentials and yields a fitted value for the forward, coherent slope of 59.0 $\pm$ 1.4 GeV^{-2}.

Figure 5 shows the $\pi^+\pi^-$ mass distribution for all diffractively produced two pion events (Figure 5a) and for the subsample of events corresponding to forward, coherent production (Figure 5b).

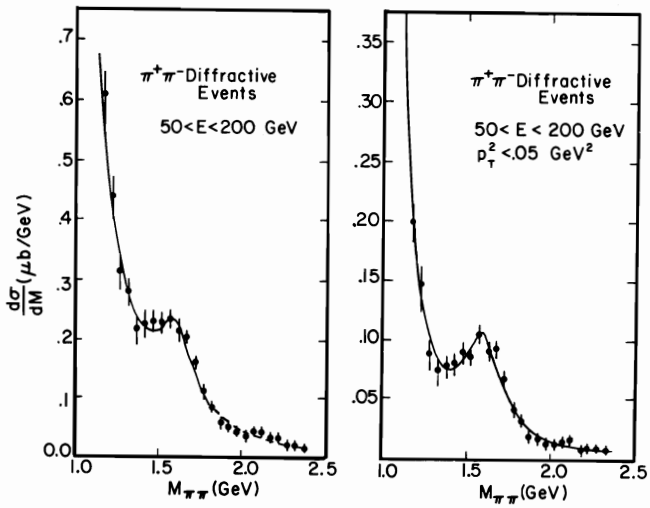

Fig. 5. The $\pi^+\pi^-$ mass spectrum for a) all events; b) for those events having $p_T^2 < 0.05$ GeV^2.

The events in Figure 5b are selected by requiring $p_T^2 <$ 0.05 GeV^2. Both mass distributions in Figure 5 indicate an enhancement in the neighborhood of 1600 MeV and illustrate that an improved signal to background ratio is obtained by selecting the forward, coherent events. The solid curves show the results of fitting the mass spectrum to the incoherent sum of a Breit-Wigner resonance and a monotonically decreasing background function. The fitted parameters of the resonance are:

$$M = 1600 \pm 10 \text{ MeV}; \quad \Gamma = 283 \pm 14 \text{ MeV} \qquad (1)$$

The errors quoted here are purely statistical. Although the central values of the parameters are insensitive to the assumptions made about the background, the errors in the parameters show some dependence on the choice of the form used for the background. An additional uncertainty of 40 MeV in both the mass and the width of the resonance results from the uncertainties associated with the form used for the incoherent background function.

The fitted parameters can be used to determine a cross section for this enhancement at 1600 MeV. The total integrated cross section is:

$$\sigma(\gamma C \rightarrow \rho'' C \rightarrow \pi^+\pi^- C) = 67 + 33 \text{ nb/nucleon} \qquad (2)$$

where the error is totally dominated by systematic effects, such as uncertainties in the triggering efficiency.

An analysis of the photoproduced 4 π mass spectrum in the region around 1600 MeV and a comparison of the $\pi^+\pi^-$ and 4 π distributions is presented later in this paper. Indications for the existence of the two pion decay mode of the ρ" (1600) have been reported previously in an earlier high energy photoproduction experiment [1] and a state with the same quantum numbers and a similar mass and width has been identified in a $\pi^+-\pi^-$ scattering phase shift analysis of the reaction $\pi p \to \pi^+\pi^- n$. [4]

$\bar{p}p$ Final State

Results on the photoproduction of $\bar{p}p$ final states have been submitted to the Symposium by two low energy track chamber experiments. These results are interesting to examine for structure in the $\bar{p}p$ invariant-mass spectrum because resonances in this channel have been reported by experiments using hadron beams. [5]

The first of the two low energy, track chamber experiments was performed at the Cornell University Electron Synchrotron [6] and measured the dependence of the $\bar{p}p$ virtual-photoproduction cross section on s (the invariant mass squared of the hadronic final state) and Q^2 (the four-momentum-transfer squared) by studying the reaction:

$$ep \to epp\bar{p} \qquad (3)$$

The analysis of this reaction yielded a sample of between 64 and 48 events, depending upon the details of the geometric cuts that were used. While the sample size is very small, it is believed to be very clean with less than 10% contamination from background events. Because of the limited statistics, results on the $\bar{p}p$ virtual photoproduction cross section are presented only for all s as a function of Q^2 and for all Q^2 as a function of s. The results are summarized in Table 1 and plotted in Figure 6.

Table 1. Virual-photoproduction cross sections for $ep \to epp\bar{p}$.

$\langle s\rangle = 11.9$ GeV^2		$\langle Q^2\rangle = 1.48$ GeV^2	
Q^2(GeV^2)	σ (nb)	s(GeV^2)	σ(nb)
1.06	84+28	9.5	15+ 6
1.83	16+6.8	11.1	36+11
2.70	6.4+4.7	112.8	36+18
		15.0	50+30

In addition to the indicated statistical uncertainties, there are uncertainties in the overall normalization at about the 25% level.

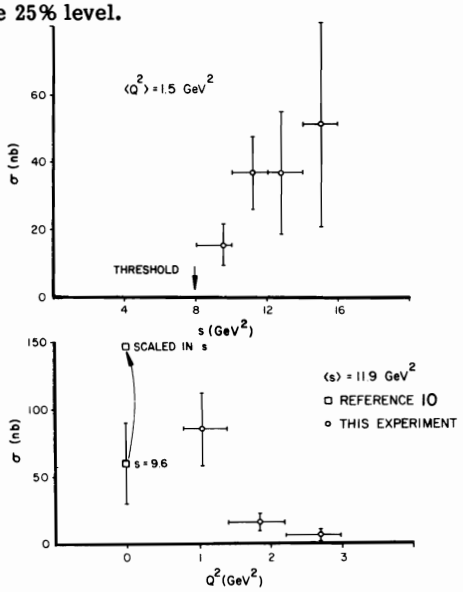

Fig. 6. Cross section for the reaction $\gamma p \to pp\bar{p}$ a) as a function of p for all Q^2; b) as a function of Q^2 for all s.

The results in Figure 6(a) indicate that the cross section rises rapidly above threshold after which it is consistent with being flat in s. The Q^2 dependence of the cross section is shown in Figure 6(b) which also includes the result from a single photoproduction measurement [7] conducted near the threshold for the reaction. The photoproduction point is shown scaled in p, using the virtual-photoproduction s dependence observed in the Cornell experiment and extrapolating to the same average s as the rest of that data. The Q^2 dependence of the cross section, including the photoproduction point, shows a steep, smooth falloff similar to that observed for other exclusive channels.

The distribution of $\bar{p}p$ invariant masses for the Cornell data is shown in Figure 7.

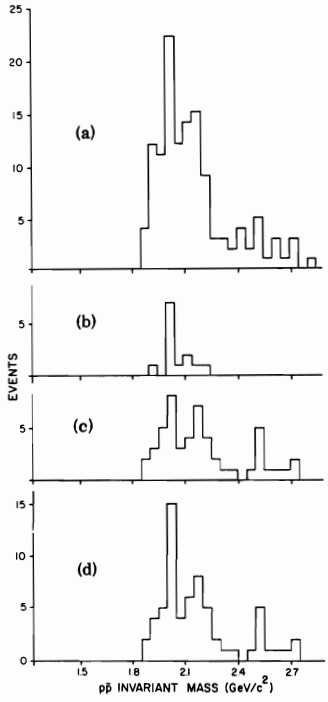

Fig. 7. The distribution of $\bar{p}p$ invariant masses for the reaction $\gamma p \to pp\bar{p}$ for a) all $\bar{p}p$ combinations; b) $\bar{p}p$ combinations having the Jackson angle nearest 90° when that angle is within ± 10° of 90°; c) $\bar{p}p$ combinations having the Jackson angle nearest 0° or 180° for all events not appearing in (b); d) the sum of b) and c).

Both possible $\bar{p}p$ pairings for each event are included in Figure 7(a), even though this produces a combinatorial background. There is a possible indication of structure in the bin from 2.00 to 2.05 GeV, a region in which a resonance has been previously reported. [5] Figure 7(b) attempts to reduce the influence of the combinatorial background by plotting the invariant mass for those events and $\bar{p}p$ pairings which produce Jackson angles (the angle between the target proton and decay proton in the $\bar{p}p$ center of mass) in the interval 90°±10°. In Figure 7(c) the remaining events are shown assuming the combination which produces a Jackson angle nearest 0° or 180°. Figure 7(d), which is the sum of 7(b) and 7(c), contains each event exactly once and has a reduced combinatorial background.

The experimenters have analyzed the mass spectrum of Figure 7(D) and have attempted to estimate the masses, widths and virtual-photoproduction cross sections for the two possible resonant states at 2.02 and 2.20 GeV^2. The results are summarized in Table 2.

Table 2. $\bar{p}p$ resonance summary for the reaction $ep \rightarrow ep\bar{p}p$

Mass(GeV)	FWHM(GeV)	Number of Events	σ (nb)
2.02	< 0.040	12+4.0	6.6+2.2
2.20	≈0.060	9±4.5	5.0±2.5

The uncertainties in these estimates of the virtual-photoproduction cross section are purely statistical. In addition to the overall normalization uncertainties of 25%, mentioned earlier, there are systematic uncertainties which could be as large as 30%. Neither of the two indications for resonant structure, shown in Figure 7(d) and summarized in Table 2, has a statistical significance greater than three standard deviations; however the masses at which these indications appear agree well with resonances previously reported to exist at 2.02 and 2.20 GeV [5]. It is interesting to note that if these resonances are really present at the apparent levels, they account for approximately one-third of the observed $\gamma_v p \rightarrow ppp$ cross section.

The second low-energy, track chamber experiment was performed at NINA by a group from Daresbury and made use of a real photon beam to measure the invariant mass spectrum of photoproduced $\bar{p}p$'s from threshold to a maximum beam energy of 4.8 GeV.[8] Time of flight information is exploited to perform a 4-C fit to the reaction:

$$\gamma p \rightarrow pp\bar{p} \qquad (4)$$

As in the case of the Cornell experiment, the event sample size is small but rather free from background and the combinatoric ambiguity arises on the appropriate pairing of the proton and anti-proton. The results are illustrated in Figure 8.

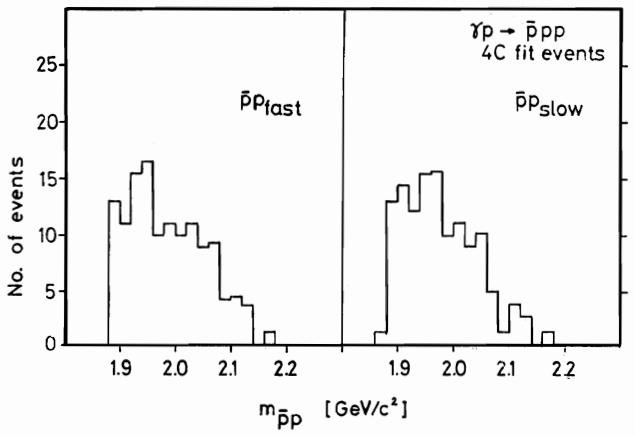

Fig. 8. The $\bar{p}p$ invariant mass spectrum in the reaction $\gamma p \rightarrow ppp$ for a) pairings of the anti-proton with the fast proton b) pairings of the anti-proton with the slow proton.

Each event makes one contribution to Figure 8(a), which shows the result of pairing the anti-proton with the fast proton and to Figure 8(b), which illustrates the result of pairing the slow proton and the anti-proton. The result of combining Figures 8(a) and 8(b) together is shown in Figure 9(a).

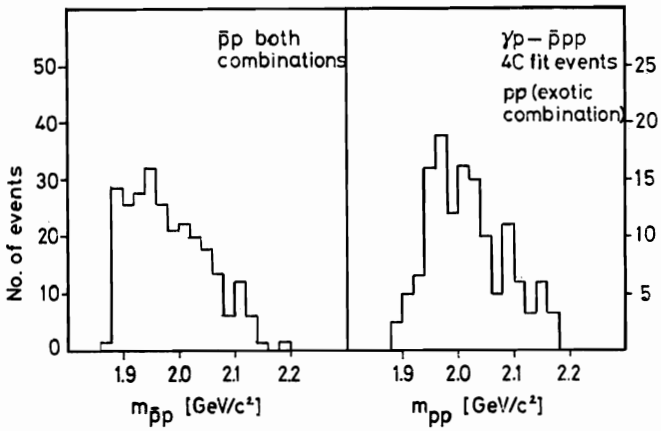

Fig. 9. The invariant mass spectrum in the reaction $\gamma p \rightarrow pp\bar{p}$ for a) both possible pairings of the proton and anti-proton b) for the pairing of the two protons.

For comparison purposes, Figure 9(b) shows the mass spectrum of the "exotic combination" which results from the pairing of the two protons. The experimenters conclude that there is no clear evidence of any narrow resonance production.

A high statistics experiment on $\bar{p}p$ photoproduction is clearly desirable.

Four-Body Final States

Four-Pion State

The four pion final state has been studied extensively in both e^+e^- annihilation[9,10] and photoproduction experiments[11,12]. The mass spectrum indicates a broad enhancement, the $\rho''(1600)$ whose reported mass varies between 1430 and 1620 MeV and whose reported width varies from 310 to 650 MeV.

The measurement of the two pion decay of the ρ'' (1600) photoproduced off carbon in the broad band beam, which was described above, was also accompanied by a measurement of the $\pi^+\pi^-\pi^+\pi^-$ final state. The distribution of events as a function of p_T^2 is shown in Figure 10.

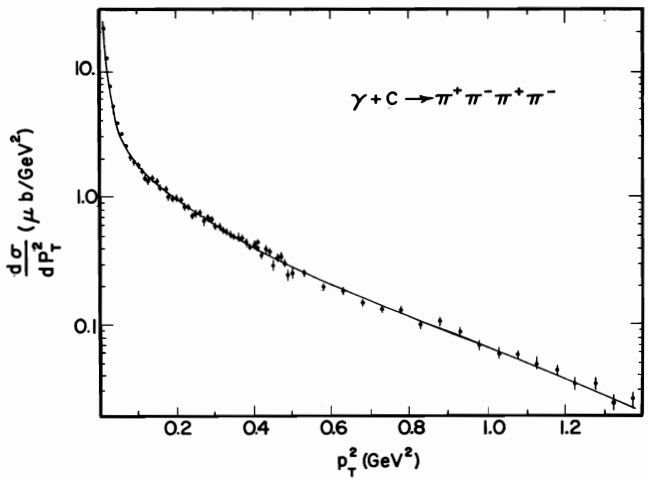

Fig. 10. The p_T^2 distribution for exclusively produced four pion final states.

The p_T^2 distribution for the four pion events is extremely similar to that of the two pion events shown earlier in Figure 4. The solid curve shown in Figure 10 represents the result of fitting the distribution to the sum of three exponentials and yields a fitted value for the forward, coherent slope of 64.6 ± 0.6 GeV^{-2}.

Figure 11 shows the $\pi^+\pi^-\pi^+\pi^-$ mass distribution for all exclusively photoproduced four pion events (Figure 11a) and for the subsample of events corresponding to forward, coherent production (Figure 11b).

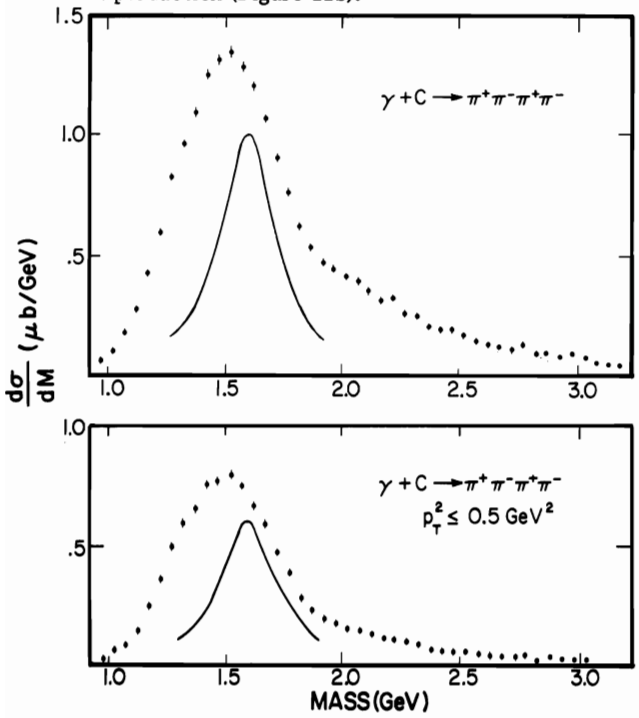

Fig. 11. The $\pi^+\pi^-\pi^+\pi^-$ mass spectrum for a) all events; b) for those events with $p_T^2 < 0.05$ GeV^2. The solid curves are Breit-Wigner distribution with a mass of 1600 MeV and a width of 283 MeV.

The events in Figure 11(b) are selected by requiring $p_T^2 < 0.05$ GeV^2. Both mass distributions in Figure 11 indicate an enhancement in the neighborhood of 1600 MeV, but an enhancement whose shape and width appears to be significantly different from those observed in the two pion distribution. This difference is illustrated with the solid curves shown in Figure 11 which are Breit-Wigner distributions with the mass and width determined from the enhancement in the two pion final state.

This difference between the two pion and four pion mass distributions in the neighborhood of 1600 MeV persists even when one restricts the four pion events to those which consist of $\rho^0\pi^+\pi^-$, since only 20% of the events fail to satisfy this criterion. The four pion final state appears to be dominated by the production of a low mass pion pair accompanied by a ρ^0 meson. Figure 12 shows the mass distribution for the lowest mass $\pi^+\pi^-$ pair within the event (Figure 12A) and the mass distribution for the pion pair opposite this low mass pair (Figure 12b).

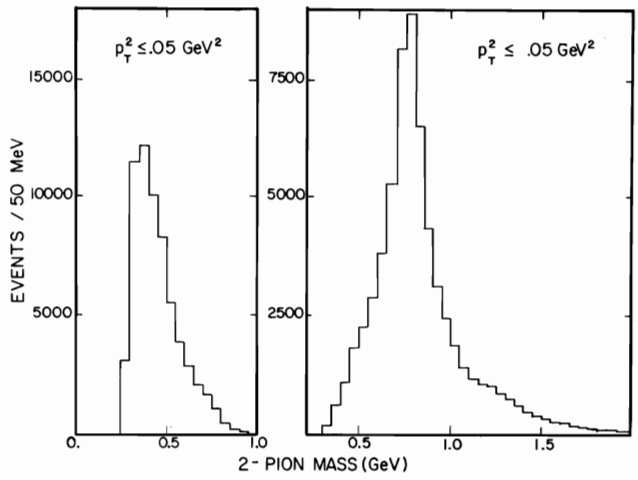

Fig. 12. The mass distribution of a) the lowest mass $\pi^+\pi^-$ pair within the four pion events shown in Figure 11b; b) the pion pair opposite the pair entered into a).

The total cross section obtained by integrating over the four pion mass distribution is:

$$\sigma(\gamma C \rightarrow \pi^+\pi^-\pi^+\pi^- C) = 1.02 \pm 0.15\ \mu\text{b/nucleon} \qquad (5)$$

In summary, enhancements in the neighborhood of 1600 MeV are observed in both the photoproduced $\pi^+\pi^-$ final state and the $\pi^+\pi^-\pi^+\pi^-$ state. However the shapes and widths of the two enhancements are quite different, most likely indicating that a number of processes are contributing to the structure of the enhancement in the four pion final state. Clearly a great deal of additional work is needed to clarify the details of what is going on in the 1600 MeV region.

$K^+K^-\pi^+\pi^-$ Final State

The evidence for the existence of high mass isovector states provides compelling motivation for a search for photoproduced high mass isoscolar states. In analyzing the data from the broad band beam we have concentrated on final states that might provide evidence for an excited ϕ^0 meson, the ϕ'. Good candidates for such final states are $K^+K^-\pi^+\pi^-$, $K^+K^-\rho^0$, $K^*K^\pm\pi^\mp$ and $\phi^0\pi^+\pi^-$. The good particle identification and the large forward acceptance of the broad band beam spectrometer make these states easily accessible.

The mass distributions for the $K^+K^-\pi^+\pi^-$ and $K^+K^-\rho^0$ final states, exclusively photoproduced off carbon, are shown in Figure 13 and for the $K^*K^\pm\pi^\mp$ and $\phi^0\pi^+\pi^-$ final states in Figure 14.

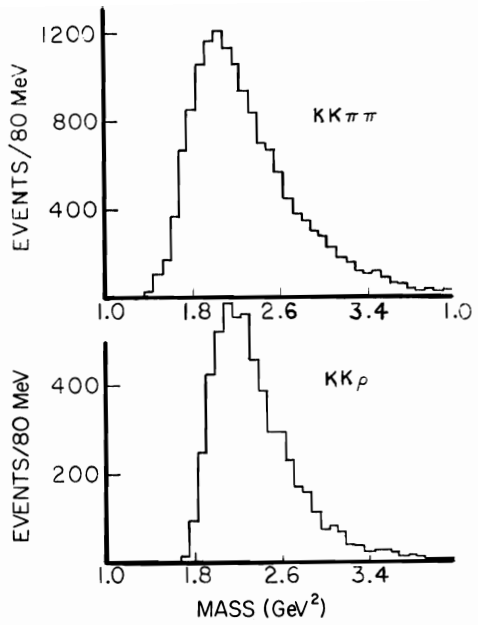

Fig. 13. The mass distributions of the exclusively photoproduced final states a) $K^+K^-\pi^+\pi^-$ and b) $K^+K^-\rho^o$.

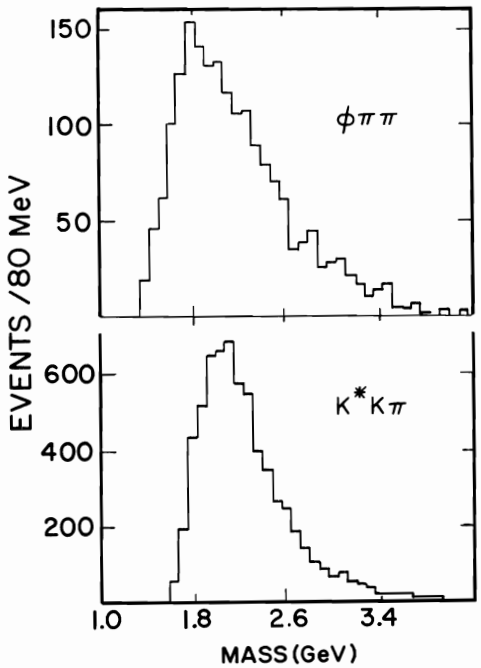

Fig. 14. The mass distributions of the exclusively photoproduced final states a) $K^+K^-\rho^+$ and b) $\phi^o\pi^+\pi^-$.

The mass distributions for all four final states shown in Figure 13 and 14 are quite smooth and present no evidence of resonant structure below 3.0 GeV. It is reasonable to expect that the sensitivity for observing ϕ' associated states would be enhanced by imposing diffractive requirements on the states shown in Figures 13 and 14. Such requirements did provide improved sensitivity for the observation of the decay $\rho'(1600) \to \pi^+\pi^-$ (Figure 5). Figure 15 shows the results of selecting the forward, coherently produced $K^+K^-\pi^+\pi^-$ and $K^+K^-\rho^o$ events.

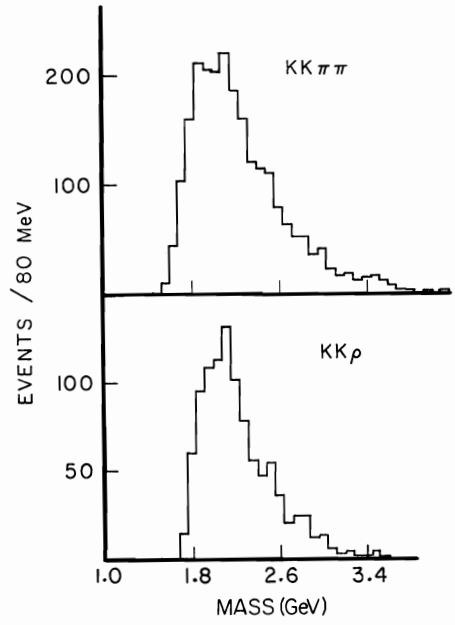

Fig. 15. The mass distribution of forward, coherently produced a) $K^+K^-\pi^+\pi^-$ events and b) $K^+K^-\rho^o$ evemts.

No structure is observed in the distributions of Figure 15. In order to calculate a limit on the product of the cross section and branching ratio for these states, a 150 MeV width has arbitrarily been assumed, and consequently events from two 80-MeV wide bins in Figure 15 are taken for the background. The cross section times branching ratio limit is calculated for a three standard deviation fluctuation in the highest bin. With a 95% confidence level the upper limits for coherent production are:

$$\sigma(\gamma C \to \phi' C) \times \frac{\Gamma(\phi' \to K^+K^-\pi^+\pi^-)}{\Gamma(\phi' \to K^+K^-\rho^o)\ \Gamma(\phi' \to K^*K\pi)\ \Gamma(\phi' \to \phi^o\pi^+\pi^-)} < 15 \text{ nb} \qquad (6)$$

Tests of the OZI Rule

The $K^+K^-\pi^+\pi^-$ final state is an interesting one to use in a test of the applicability of the quark-line (Okubo–Zweig-Iizuka) rule to photon induced reactions. Previous tests of the OZI rule have compared the relative rates of ω^o and ϕ^o production in various exclusive channels using pion, proton and anti-proton beams.[13,15] These exclusive hadroproduction experiments have found generally good agreement with OZI expectations, the production rates for the processes forbidden by the OZI rule typically being no more than 2% of that of the allowed channels. Similar tests with photon induced reactions can be used to obtain additional information on whether the rule has validity for production reactions as well as decay processes.

Two quark-line diagrams for $\phi^o\pi^+\pi^-$ photoproduction are shown in Figure 16.

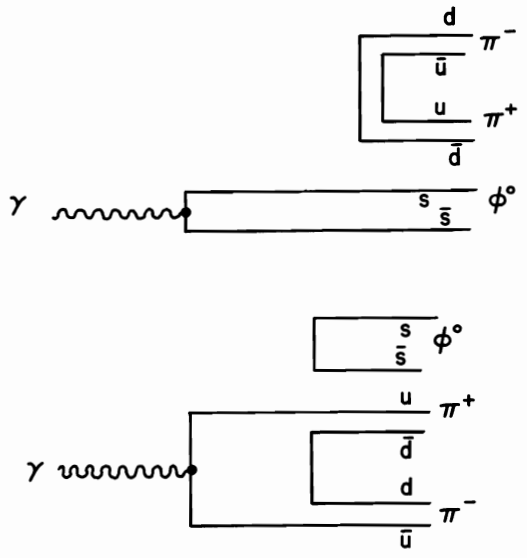

Fig. 16. Possible quark-line diagrams for $\phi^0\pi^+\pi^-$ photoproduction.

Both of the diagrams shown in Figure 16 are disconnected and therefore OZI suppressed. The sample of $\phi^0\pi^+\pi^-$ events, used in searching for evidence of the ϕ' meson, can be used to determine the degree of suppression, if any. We compare the rate of $\phi^0\pi^+\pi^-$ production with that of $\omega^0\pi^+\pi^-$ since the quantum numbers for these states are the same and the difference in available phase space is quite small. The result obtained for the relative rates of $\phi^0\pi^+\pi^-$ and $\omega^0\pi^+\pi^-$ production in the broad band beam experiment are:

$$\frac{\sigma(\gamma C \to \phi^0\pi^+\pi^- C)}{\sigma(\gamma C \to \omega^0\pi^+\pi^- C)} = .97 \pm .019 \qquad (7)$$

this result is considerably larger than what has been observed in the hadroproduction experiments (2%) and consequently represents less suppression than has been seen in the production of these states by hadrons.

One significant difference between the $\phi^0\pi^+\pi^-$ and $\omega^0\pi^+\pi^-$ final states is that the former contains two strange quarks, while the latter contains only non-strange quarks. It is therefore of interest to compare the yield of $\phi^0\pi^+\pi^-$ to that of $K^+K^-\pi^+$ and $K^+K^-\rho^0$. Each of these states is observed by detecting the same final four particles, two kaons and two pions, and all three states contain a vector meson and two pseudo-scalors. The measured ratios are:

$$\frac{\sigma(\gamma C \to \phi^0\pi^+\pi^- C)}{\sigma(\gamma C \to K^{*}K^{\pm}\pi^{\mp} C)} = 0.35 \pm 0.07 \qquad (8)$$

and:

$$\frac{\sigma(\gamma C \to \phi^0\pi^+\pi^- C)}{\sigma(\gamma C \to K^+K^-\rho^0 C)} = 0.68 \pm 0.14 \qquad (9)$$

In comparing states with the same number of strange quarks, no large suppression is observed in the yield of the $\phi^0\pi^+\pi^-$ state, the only one with a disconnected diagram.

In summary, the degree of suppression of the $\phi^0\pi^+\pi^-$ final state in photoproduction reactions appears to be significantly less than in hadroproduction experiments. This may well indicate that all disconnected quark-line diagrams are not equally surpressed; however, it appears that in photon induced reactions one does not observe the full suppression expected from a naive application of the OZI rule.

Photoproduction of Charmed Mesons

The upgrade of the broad band beam spectrometer to include the ability to identify heavy particles was motivated by a search for the photoproduction of $D^0\bar{D}^0$ pairs. The exposure for this run consisted of 10^{17} incident primary protons which produced 6×10^{11} photons with energies greater than 50 GeV. In order to help suppress the background induced by K_L^0's in the neutral beam, the event sample which has been selected for analysis was required to contain one K^+ and one K^- with no other identified heavy hadron in the event. In the same spirit, to help suppress the background from neutrons in the neutral beam, the events are required to have a total visible energy of less than 200 GeV. An additional requirement is that the K^+K^- mass fall outside the range 1.01 - 1.03 GeV, i.e., that they do not form a ϕ^0 meson.

With this event sample we have examined the $K^{\pm}\pi^{\mp}$, $K^+K^-\pi^+\pi^-$ and $K^0_S\pi^+\pi^-$ final states for evidence of the D^0 ($\bar{D}^0$) mesons. To keep the number of combinations in the event from growing too large, we make the further restriction that the total number of pions in the event be at most three larger than the number of pions in the combination. Subject to these requirements, the only signal we have found near the known D mass with a statistical significance greater than four standard deviations appears in the $K^-\pi^+$ decay mode of the D^0 ($\bar{D}^0$). This mass distribution is shown in Figure 17(a) along with a best fit to a smooth background plus a superimposed Gaussian.

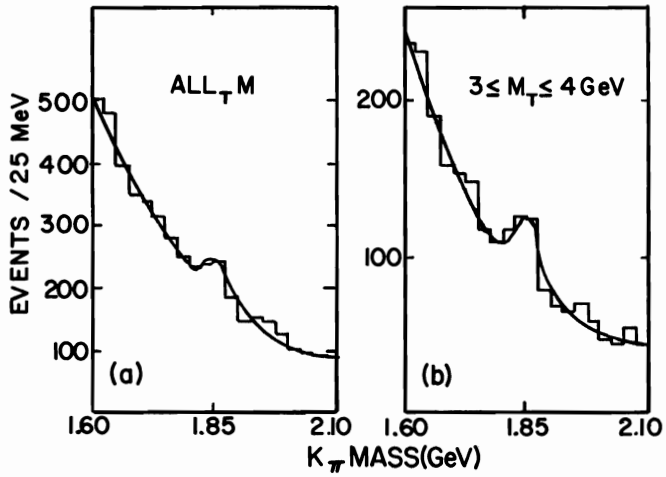

Fig. 17. The $K^{\pm}\pi^{\mp}$ mass distribution for a) all events; b) for events whose total invariant mass lies in the 3.0 - 4.0 GeV interval.

The results of the fit to the distribution shown in Figure 17(a) yields:

$$M = 1861 \pm 6 \text{ MeV}; \quad \sigma = 17 \pm 5 \text{ MeV} \qquad (10)$$

with 99 ± 24 events above background ($\chi^2 = 11$ for fourteen degrees of freedom). The calculated resolution for this state is σ (expected) = 17 MeV.

Figure 17(b) illustrates the effect of requiring that the total invariant mass visible in the event lies within the interval 3.0-4.0 GeV. The best fit to the distribution of Figure 17(b) is:

$$M = 1854 \pm 6 \text{ MeV}; \quad \sigma = 20 \pm \text{MeV} \qquad (11)$$

with 94 ± 19 events above backgrounds ($\chi^2 = 9$ for fourteen degrees of freedom). An analysis of the data taken with six radiation lengths of lead in the neutral beam indicates that the number of events above background in Figure 17(b) which are due to K_L^0 or neutron interactions is 5 ± 20.

We have relied upon Monte Carlo techniques to translate the above results into a cross section for the photoproduction of $D^0 \bar{D}^0$ pairs. The Monte Carlo model generates an intermediate $D^0 \bar{D}^0$ state with a mass of 4.0 GeV carrying the full energy of the interacting photon. The cross section for producing the intermediate $D^0\bar{D}^0$ state is assumed to be independent of energy over the interval 50-200 GeV. The D^0 is forced to decay into the $K^- \pi^+$ channel while the $\bar{D}^0$ is allowed to decay through sixteen different decay modes. In this model the $\bar{D}^0$ decay is characterized by an average charged multiplicity of 2.2 and a K^+ to $\bar{K}^0$ ratio of 57 to 43. The cross section based on this Monte Carlo model is sensitive at the 10% level to: (i) the mass of the intermediate $D^0 \bar{D}^0$ state (varied from 4.0 to 4.5 GeV) and (ii) the photon energy range used for producing this state (varied from 50 to 100 GeV threshold). The effects of these uncertainties in the model have been included in the total systematic error in the determination of the $D^0 \bar{D}^0$ cross section which we estimate to be $\pm$ 40%.

Using the model described above and a branching ratio for $D \to K\pi$ of 2.5% [16], the 94 ± 19 events of Figure 17(b) correspond to a cross section of

$$\sigma (\gamma N \to D^0 \bar{D}^0) = 520 \pm 210 \text{ nb/nucleon} \qquad (12)$$

where the error includes our estimated systematic uncertainty.

To check the internal consistency of the data we have used the $K^\pm \pi^\mp \pi^+ \pi^-$ decay mode. Figure 18 shows the mass distribution for this state subject to the same cuts as Figure 17(b).

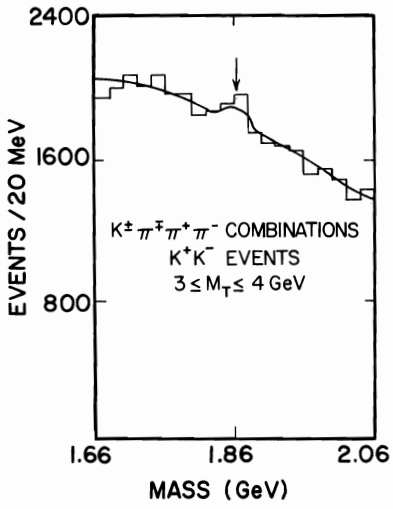

Fig. 18. The $K^\pm \pi^\mp \pi^+ \pi^-$ mass distribution.

The fitted function shown in Figure 18 consists of the incoherent sum of a polynomial background and a Gaussian with a central mass of 1.862 GeV and a width determined from a Monte Carlo calculation of the resolution for this final state.

Using a branching ratio for $D \to K\pi\pi\pi$ decay of 4.4% [22], the 177 ± 69 events above background in Figure 18 correspond to a cross section for $D^0 \bar{D}^0$ photoproduction of 525 ± 294 nb/nucleon. Even though the statistical significance of this result is not strong it does serve the purpose of providing an internal consistency check and is in excellent agreement with the result obtained from the $K^- \pi^+$ state.

In summary, the cross section for the photoproduction of $D^0 \bar{D}^0$ pairs is large: 0.5 μb/nucleon or approximately 1/2% of the total hadronic cross section.

Acknowledgements

I wish to thank my collaborators on the broad band beam experiments from Fermilab, Columbia University and the University of Illinois for their cooperation and advice in preparing this review. Conversations with D. Harding and D. H. White on the results from Cornell and with R. Marshall on the Daresbury data were enlightening and useful.

Discussion

Q. (E. Gabathuler, CERN) One year ago at the Tokyo Conference some preliminary results were presented on charmed baryon production, showing a peak in the $\Lambda 3\pi$ mass spectrum, and the problems of K_L^0 induced backgrounds. Have you any comment to make on that?

A. Yes, Let me show you a picture first. I have to find the right slide. The data that I presented here on the charmed mesons is that same data sample that was presented at Tokyo. The analysis of that data sample, over and above these results on the charmed mesons, has been going on for a year and will probably take another three or four months before we're as comfortable with it as we would like as far as three topics go. First, we would like to repeat the search for charmed mesons requiring only one K in the final state. That's something that is currently going on. Second, you notice that I had nothing to say about either K^0 or Λ^0 final states. The problem with those final states is that most of them decay in magnet M1 (Figure 2). We accept events where one of those decay products goes through the full spectrometer and the second decay product just goes through the first three chambers. In order to do that and preserve your resolution and get everything right for the case where a V^0 decays inside the magnet, it appears as though you have to do everything extremely well. Particularly, what happened in our case is that halfway through the run one of the coils in this magnet shorted out and we had not measured it beforehand. We feel we know the field integral of the magnet fairly well, but it has taken us a tremendous amount of time and effort to get a detailed field map from the data itself. We felt this was necessary before we could say anything more on final states where there's a V^0 which decays inside the magnet. That's something that a lot of work has been done on and is still being done on, but it looks like it will be another two or three months before we're in a position to come out with anything there.

Q. (T. Truong, Ecole Polytechnique) I wish, to make a comment on the funny behaviour of the $\rho \to 4\pi$. It looks funny but it's completely expected on theoretical grounds. Namely, at least in $e^+e^- \to 4\pi$ one can calculate by current algebra the background and the background is about 50% of the signal for $\rho' \to 4\pi$. The interference between background and the signal is very important and that requires a detailed analysis. This situation does not exist for the signal of $\rho' \to 2\pi$. So I would conclude from the data that the parameters for the ρ' are given by your data on $\rho' \to 2\pi$.

A. Let me see if I can understand what you've said. You're saying that even though, to the eye, you have two things, both with central mass at 1600, and that in 2π one of them looks like it's a good bit narrower than in 4π, do not be surprised and don't be disturbed, that these could be the same thing.

Q. That's right. Because in $\rho' \to 4\pi$ you have a lot of background and this background can be calculated, at least in the threshold region, by current algebra.

A. Okay. In that case, I'd like to give you our data and ask you to do it.

Q. (H. Lipkin, Weizmann/Fermilab/Argonne) I'd like to make a comment on this OZI rule. This particular experiment, I think for instance, is a very rich source of information for understanding the OZI rule because there are two kinds of diagram. If you could show that transparency (Figure 16). There's been some confusion about what is forbidden and what isn't. From this you can see that the diagram in Figure 16(a) makes use of the ss that is already in the photon, whereas the diagram in Figure 16(b) does not. My feeling is that you get less suppression from the first diagram. This actually shows up in data. For example, if you look at $\phi 2\pi$, $\phi 3\pi$ and $\phi 4\pi$ you find a striking systematic effect in that the $\phi 4\pi$ looks like the $\phi 2\pi$ but the $\phi 3\pi$ is much lower. Now the first diagram is forbidden for $\phi 3\pi$ by G-parity, so that if you could also look at omegas withoug a number of pions, which you can't without detecting π^0, and compare it with the phi's you could get some nice systematics. Also, the ratio of $\omega K\bar{K}$ and $\phi K\bar{K}$ to $\rho K\bar{K}$ is very interesting in this context.

Q. (G. Kalmus, Rutherford Lab) Could you tell me whether you have any hopes of getting a cross section for charm production with photons, say, between 20 and 50 GeV, since you clearly have very many more photons in that energy range than above 50 GeV?

A. No. We wouldn't even try. Our acceptance there for a multibody final state is very low.

Q. (R. Galik, Univ. Of Penn.) Do you have an angular distribution from the 2π final state of the ρ'?

A. It looks the same both on and off resonance in the same way that the t-distrubution looks the same both on and off resonance. I don't have it with me to show you, but it doesn't seem to shed any light on things.

References

1. W. Lee, proceedings of the 1975 International Symposium on Lepton and Photon Interactions at High Energies, W. T. Kirk, editor (SLAC 1975).
2. W. Lee, Proceedings of the 1977 International Symposium on Lepton and Photon Interactions at High Energies, F. Gutbrod, editor (Hamburg, 1977).
3. A. Eisner, these proceedings.
4. B. Hyams et. al., Nucl. Phys. B64, 134 (1973)
5. P. Benkheiri et. al., Phys. Lett. 68B, 483 (1977).
6. B. G. Gibbard et. al., Phys. Rev. Lett. 42, 1593 (1979).
7. J. Ballam et. al., Phys. Rev. D5, 545 (1972).
8. R. Marshall, private communication.
9. M. Conversi et. al., Phys. Lett. B52, 493 (1974)
10. F. Ceradini et. al., Phys. Lett. B43, 341 (1973).
11. M. Davies et. al., Nucl. Phys. B58, 31 (1973).
12. G. Alexander, Phys. Lett. B57, 487 (1975).
13 R. A. Donald et. al., Phys. ett. 61B, 210 (1976).
14. D. S. Ayres et. al., Phys. Rev. Lett. 32, 1463 (1974).
15. V. B. Cobel et. al., Phys. Lett. 59B, 88 (1975).
16. J. Kirkby, these proceedings. The cross section reported here in equation (12) differs from the result reported by M. S. Atiya et. al., Phys. Rev. Lett. 43, 414 (1979) solely because of this new measurement of the branching ratio.
17. J. Kirkby, these proceedings. The cross section reported here for the $K^{\pm}\pi^{\mp}\pi^{+}\pi^{-}$ final state differs from the result reported by M. S. Atiya et. al., Phys. Rev. Lett. 43, 414 (1979) solely because of this new measurement of the branching ratio.